PROCEEDINGS, 46th Workshop on Geothermal Reservoir Engineering
Stanford University, Stanford, California, February 15-17, 2021
SGP-TR-218

A DAS-VSP study around the geothermal field of the Ohnuma geothermal power plant in northern Honshu, Japan

Junzo Kasahara[1,2], Yoko Hasada[1,3], Haruyasu Kuzume[1], Hitoshi Mikada[4], and Yoshihiro Fujise[5]

[1]ENAA Toranomon Marine Building 10th, 3-18-19 Toranomon, Minato-ku, Tokyo 105-0001, Japan

[2] Shizuoka Univ., Center for Integrated Research and Education of Natural Hazards, 836 Ohya, Shizuoka 422-8529, Japan

[3] Daiwa Exploration and Consulting Co. Ltd., 5-10-4 Toyo, Koto-ku, 135-0016, Tokyo, Japan

[4]Kyoto Univ., Department of Earth Resources Engineering, Katsura, Nishikyo-ku, Kyoto 615-8540, Japan

[5]WELMA Co. Ltd., 2-3-3, Watanabe Street, Chuo-ku, Fukuoka 810-0004, Japan

kasahara.junzo@shizuoka.ac.jp

Keywords: Ohnuma geothermal power plant, distributed acoustic sensing, stacking, reflected phases, vertical seismic profiling, reverse-time migration supercritical water

ABSTRACT

We carried out a third geothermal seismic study using distributed acoustic sensing (DAS) at the Ohnuma geothermal power plant owned by Mitsubishi Materials Corporation in September 2020. The Ohnuma geothermal power station, the third commercial geothermal power plant in Japan, was completed in 1974; its installed capacity is 9.5 MW. We installed an optical fiber system for the distributed temperature sensor (DTS) and DAS measurements and 26 surface seismometers on the surface of the site. We deployed the optical fiber system down to a depth of 1,973 m in the O-13R borehole. The temperature was measured as 240 °C at around 1,130 m depth using the DTS mode. We operated an IVI EnviroVibe seismic source at nine locations. We repeated the frequency sweep of 10–75 Hz 480 times a day for nine days. To enhance the signal to noise ratio (S/N), we stacked the DAS data and correlated the seismic records with the source signature. By stacking for a long duration, we obtained excellent DAS records down to the bottom of the boreholes. Using the migration of observed and synthetic DAS seismic records, we recognized intense seismic reflections from 2.8–3.0 km depth, suggesting the possibility of geothermal reservoirs. The velocity decrease in this zone might be more than 1 km/s, probably suggesting the presence of a fracture zone filled with fluid. Through two field studies, conducted in the Medipolis and Ohnuma geothermal fields in Japan, the DAS seismic method in the borehole could efficiently image seismically reflective zones that suggest a high possibility of geothermal reservoirs.

1. INTRODUCTION

The New Energy and Industrial Technology Development Organization (NEDO) in Japan has promoted the use of supercritical water for geothermal power generation under a project called "Research and Development of Supercritical Geothermal Resources." Recently, fiber optics sensing technologies enabled us to use optical fiber for seismic measurement. The seismic measurement with optical fiber is called distributed acoustic sensing (DAS) (Hartog, 2017). DAS uses Rayleigh scattering of incident laser light by strain through an optical fiber. Using DAS for earthquake monitoring (*e.g.,* Lindeley *et al.,* 2017; Wang *et al*., 2018) and geothermal studies (*e.g.,* Mellors *et al.*, 2018; Trainor-Guitton *et al*., 2018), it was demonstrated that the application of fiber optics for seismic measurement is beneficial. We also used optical fiber sensing for our geothermal studies. We have studied a seismic approach using active seismic sources, DAS, and distributed temperature sensor (DTS) using fiber optics and full waveform inversion (FWI) methods to develop the most effective tools for obtaining the characteristics of geothermal fields. As a part of this program, we have focused our efforts on studying the seismological approach using DAS in the geothermal area since 2017. In 2018 and 2019, we carried out a DAS seismic survey using one of the boreholes in the Medipolis geothermal field in Kyushu Island, Japan (Kasahara *et al*., 2019a, b, 2020a). The maximum temperature measured by the DTS mode of the optical fiber was approximately 272 °C at a depth of 910 m. We obtained excellent DAS seismic records for both natural earthquakes and seismic vibrator activations. A relatively small seismic source (IVI MiniVib) was used for the active seismic experiment. We stacked the DAS data 480–960 times to enhance the signal to noise ratio (S/N) with source signature correction. By analyzing borehole DAS data, we constructed a 2D seismic velocity profile. We estimated three major hydrothermal layers at 800–1,000 m, 1,500–1,700 m, and 4,000 m depths. The zone around 3.8 km with high Vp/Vs suggests a probable fluid layer (Kasahara *et al*., 2020b).

To prove the effectiveness of our approach in other geothermal fields, we carried out a third geothermal seismic study using the DAS system at the Ohnuma geothermal power plant owned by Mitsubishi Materials Corporation in September 2020. The Ohnuma geothermal field is located in the Tohoku area of Japan (Fig. 1). The power plant is the third commercial geothermal power plant in Japan, completed in 1974, with an installed capacity of 9.5 MW. We placed an optical fiber system for the DTS and DAS measurements down to a depth of 1,973 m in the O-13R borehole and 26 surface seismometers on the surface of the site (Fig. 1).

Because the source power of the previous experiment was not large enough to detect the deeper seismic reflection from geothermal resources, we used 2.5 times larger seismic force as IVI EnviroVibe than the previous IVI MiniVib in 2019, at nine locations (Fig. 1). We repeated the frequency sweeps of 10–75 Hz 480 times (8 h operation) per day for nine days. As in the previous experiment, we stacked the observed DAS seismic data and correlated them to the source signature to enhance the S/N. The DAS seismic data in the O-13R for nine source locations were obtained by the DAS interrogators of Schlumberger Co. Ltd. and AP sensing Co. Ltd. for C1–C8 and C10B, respectively. We compared two sets of DAS data for the C8 source and confirmed that the data were almost identical. The gauge length for all DAS data was approximately 10 m, and the sampling rate was 1 ms.

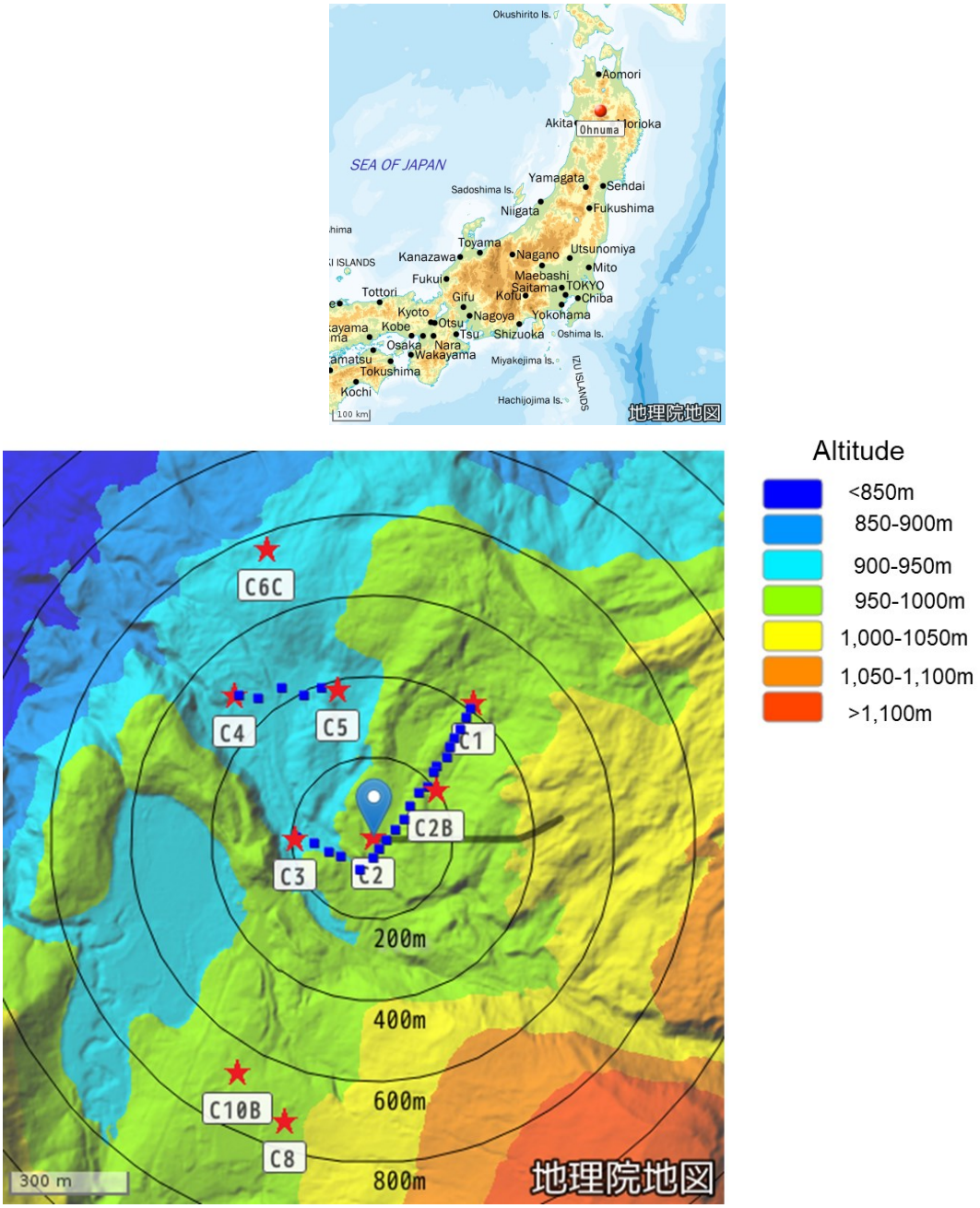

Figure 1:（Upper） Location map of Ohnuma geothermal power station (red circle). (Lower) Location map of sources (red stars), surface seismometers (blue squares), and DAS in the O-13R borehole (thick black line) around the Ohnuma geothermal power station. The O-13R borehole extends from the west to the east. Concentric circles of the radii are drawn every 200 m from the center at the wellhead of the O-13R borehole. The map by the Geospatial Information Authority of Japan is used.

2. GEOLOGICAL SETTING OF THE TEST FIELD

The Ohnuma geothermal area is located in the northern part of the Hachimantai geothermal field. The area is composed of Quaternary volcanics and thick Tertiary sediments (Kubota, 1985). The geological data in the Ohnuma geothermal power plant were obtained from the cuttings produced during borehole drilling (Yora *et al*., 1973, 1976, 1977; Kubota, 1985, Kubota *et al*., 1989). A summary of the geological section of the test field is shown in Fig. 2. The layer between a few hundred meters and 1,000 m comprises dacitic lapilli tuff. The layer between 1,000 m and 1,500 m contains altered andesite. The layer below 1,500 m is siliceous shale. Because most of the boreholes in the Ohnuma geothermal power station are shallower than 2,100 m depth, the geology of the layers present at a depth greater than 2,100 m is not known. The current geothermal production zones are located at approximately 1,200–1,700 m depth. Fig. 3 (Kubota, 1988) shows the geothermal summary of the Ohnuma-Sumikawa geothermal field. Sumikawa is another geothermal power plant. The hot area is centered at Sumikawa and Ohnuma.

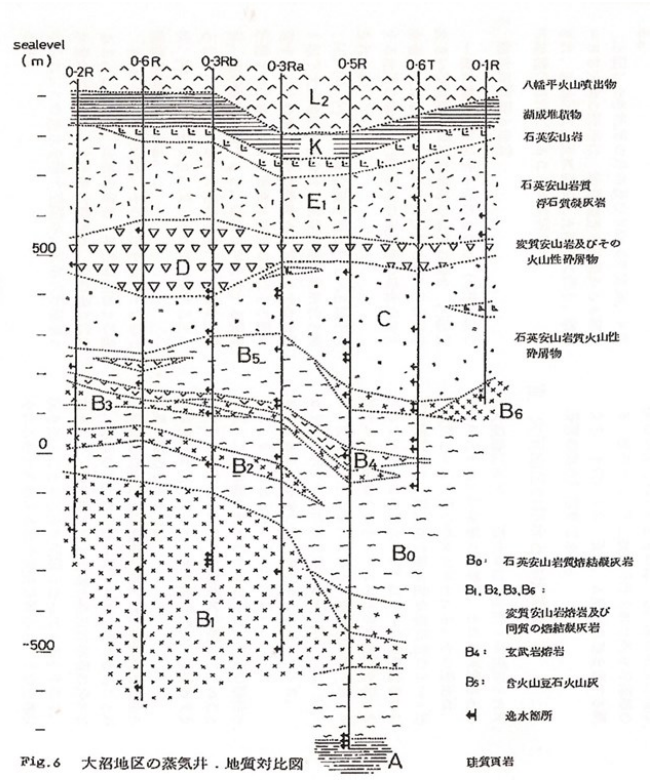

Figure 2: Geological description of the study area based on the cuttings of seven boreholes (O-2R, O-6R, O-3Rb, O3-Ra, O-5R, O-6T, and O-1R) (After Yora *et al.*, 1973). L: andesitic lava; K: siltstone; D: tuffaceous mudstone; C: dacite lava and tuff; B0 and B1: dacite welded tuff. The vertical axis is the height from sea level.

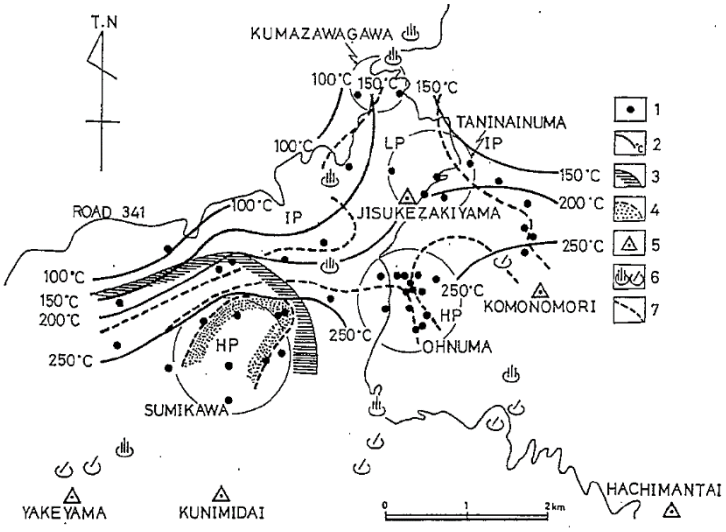

Figure 3: Geothermal outline map of Ohnuma-Sumikawa geothermal area (after Kubota, 1988). Ohnuma area is at the lower center. 1: locality of well bottom, 2: isotherm at sea level, 3: distribution area of unconsolidated lacustrine sediments, 4: vapor-dominated area, 5: volcano, 6: geothermal manifestation, 7: distribution of permeability; IP: impermeable zone, HP: permeable zone.

3. RESULTS

We obtained the temperature profile and seismic data in the O-13R borehole using a single-mode optical fiber system by DTS and DAS. The bottom of the optical fiber reached 2,037 m in length along the well, which corresponds to 1,973 m in depth.

3.1 Temperature profile in the O-13R borehole

The temperature profile is shown in Fig. 4. The maximum temperature is 240 °C at a depth of 1,130 m. This temperature profile is similar to the measurements obtained in 2016 (Mitsubishi Material personal communication). The water level is at 579 m depth.

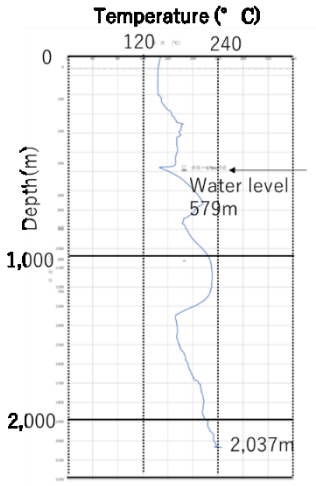

Figure 4: Temperature profile in the O-13R borehole measured by DTS mode. The water level is at 579 m. The maximum temperature is 240 °C at approximately 1,130 m depth. The vertical axis represents the depth along the well.

3.2 Separation of down-going and up-going waves using the DAS seismic data

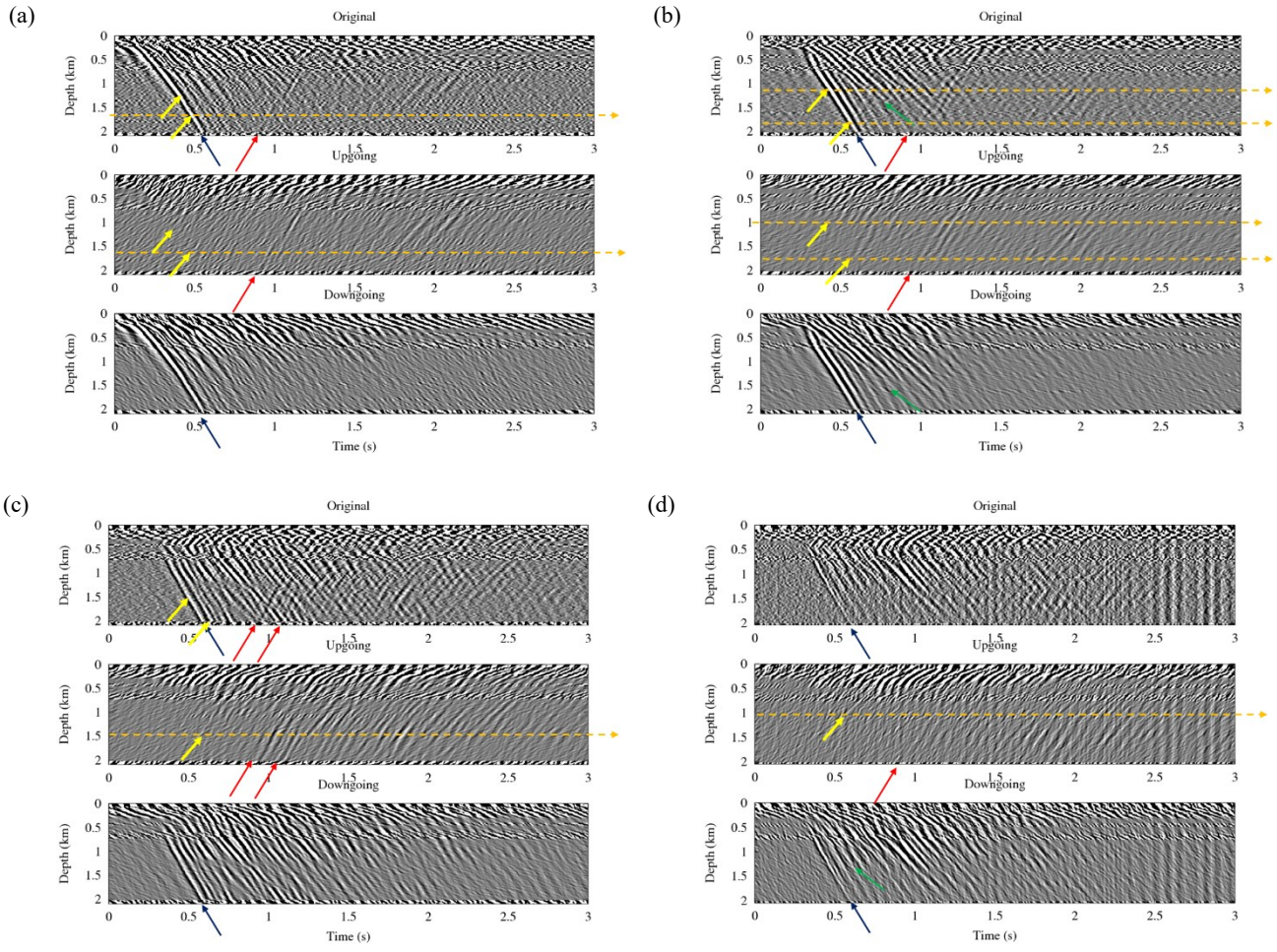

Figure 5: DAS seismic records in the O-13R borehole for C3 (a), C4 (b), C8 (c), and C10B (d). A set of three figures are original DAS records, up-going phases, and down-going phases. The vertical and the horizontal axes of each figure are depth along the well in km and travel time in s. Yellow and red arrows indicate reflected phases, and blue arrow does direct P arrival phase, respectively. Green arrows indicate the direct S arrival phase. C3 and C4 source locations are located 300 m west and 700 m north of the wellhead, respectively. C8 and C10B source locations are both located approximately 700 m south of the wellhead.

The DAS seismic data were stacked 480 times and cross-correlated with the source signature of the vibrator. Four sets of stacked DAS seismic records out of nine source locations (Fig. 1) are shown in Fig. 5. Every 5-m trace is shown in each figure. The down-going and up-going arrivals were separated from the original records using the F-K velocity filter. It is considered that the down-going and up-going phases correspond to the

direct arrivals and reflected arrivals, respectively. The direct P-wave arrivals (down-going arrivals) are shown by blue arrows. We could easily recognize the reflected arrivals at around 0.9 s arrival time (red arrows in each up-going section). This 0.9 s arrival seems to be the PP reflection from a zone around 2.8–3.0 km depth. We also recognize other P-reflected phases, shown by yellow arrows, from the layer boundaries shallower than 2 km depth. For the C8 source, we could identify two reflected arrivals around 0.9 and 1.0 s. S-wave direct arrivals are shown by green arrows. Other DAS seismic records for C1, C2, C5, and C6 have slightly weak reflected arrivals around 0.9 s.

Using the arrival times of the DAS dataset and surface seismometer, we obtained a 1-D approximate Vp profile (Fig. 6, left). The fittings of the DAS seismic records for nine source locations are shown in Fig. 6, right. Some arrivals are slightly misfitting due to horizontal heterogeneity in this area.

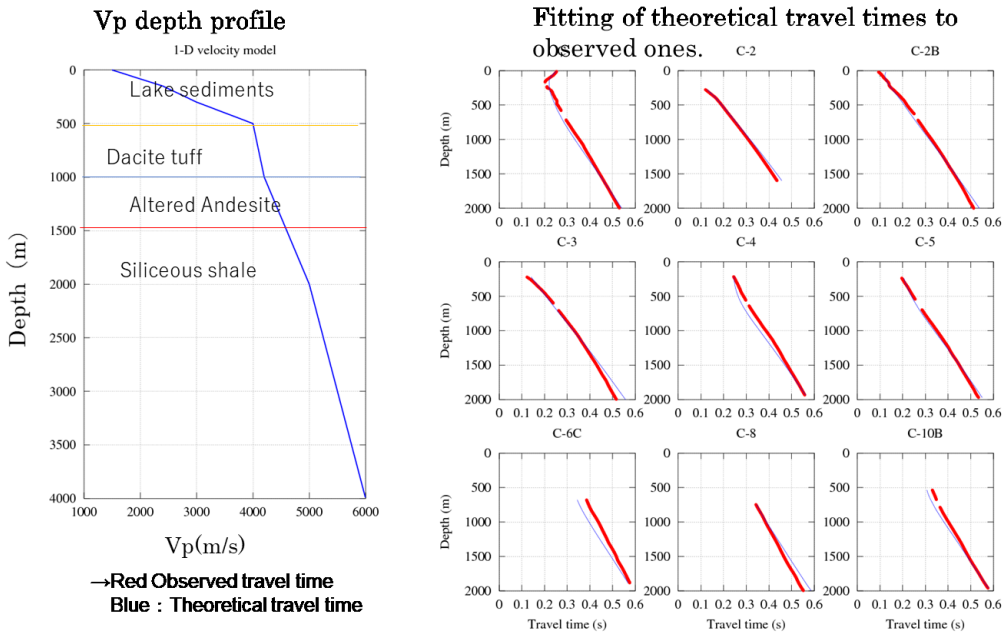

Figure 6: (Left) One-D approximate Vp depth profile using the DAS data and the surface seismometer arrivals. The change of velocity gradient at 1,000 m depth corresponds to the geological layer boundary between dacite tuff and altered andesite. The geological boundary between altered andesite and siliceous shale is not evident in the Vp depth profile. (Right) Travel time fittings for nine source excitations.

3.2 Migration of up-going waves

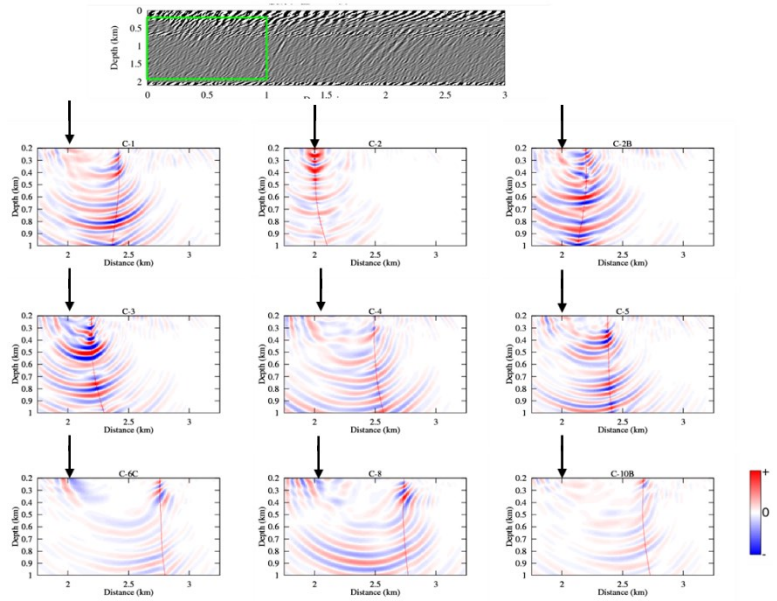

Figure 7: (Top figure) DAS section of the up-going phase for C3 seismic source. The green box shows records for migration. (Lower nine figures) results of reverse-time migration for up-going phase between 0–1.0 s arrival times shown in green box portion of the top figure. The vertical axis represents depth in km, and the horizontal one represents the distance of the locations in km. The borehole depth profile is shown in each figure as a red line. The common source location is at 2 km in each figure (black arrow).

We carried out reverse-time migration for up-going reflected phases for nine source locations using the Vp velocity model shown in Fig. 6. We separated shallower and deeper reflections at 0–1.0 and 0.75–1.5 s arrival times shown in Figs. 7 and 8, respectively. In Fig. 7, there are reflective layers at 0.5 km and 0.8 km depth. As observed from Fig. 8, there is a strong reflective zone around 2.8–3.0 km depth. Due to the small aperture of the source and DAS, the migrated sections show smiles. It seems that the zones causing reflections could exist at 0.5 km depth, 0.8 km depth, and 2.8–3.0 km depth.

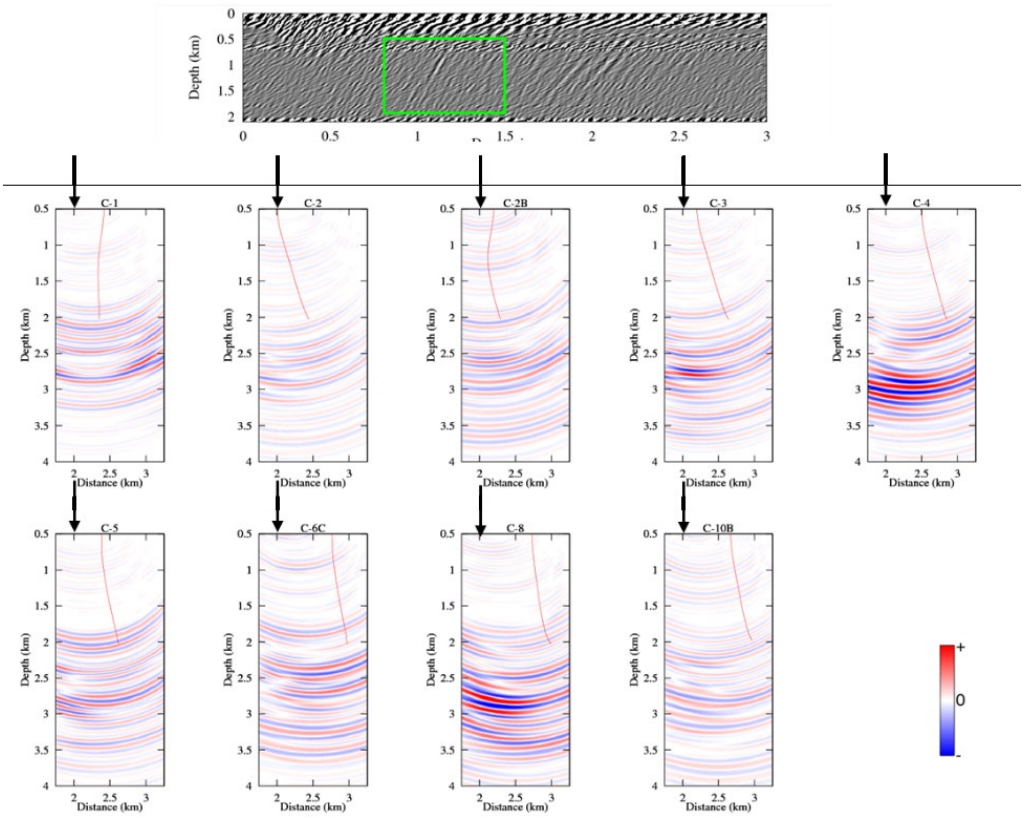

Figure 8: (Top figure) DAS section of the up-going phase for C3 seismic source. The green box shows records for migration. (Lower nine figures) Results of reverse-time migration for the up-going phase between 0.75–1.5 s arrival times are shown in the green box portion of the top figure. The vertical axis is depth in km, and the horizontal one is the distance of the locations in km. The borehole depth profile is shown in each figure as a red line. The common source location is at 2 km in each figure (black arrow). Migrated reflection zone at 2.8–3.0 km depth is the most intense for C4 and C8 and a little weak for C3.

5. SYNTHETIC WAVEFORMS

To evaluate the accuracy of our results, we calculated synthetic waveforms using the model shown in Fig. 9. The model has a small box-shaped zone with a decrease in Vp and Vs. The synthetic DAS waveforms for each source are shown in Fig. 10. The reflected phase from 2.8 km depth is not very intense. Using the up-going phases of the synthetic waveforms, we migrated the reflections (Fig. 11).

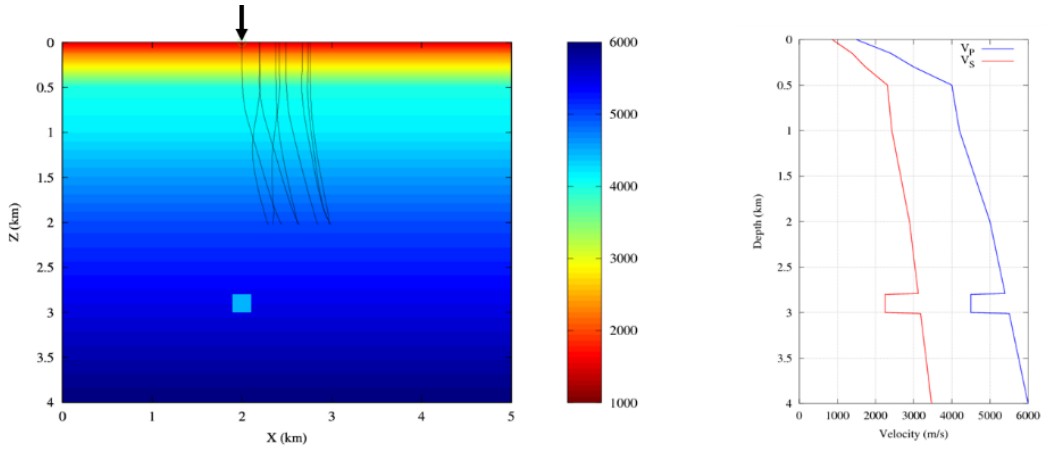

Figure 9: (Left) The structural common source model interpreting the 0.9 s reflections seen in the DAS seismic sections. The common vertical force, as a seismic source, is shown by the black arrow. (Right) Vp and Vs model used for the calculation. We place a Vp and Vs gap at 2.8–3.0 km depth with a width of 200 m. The boreholes traces are shown as black lines.

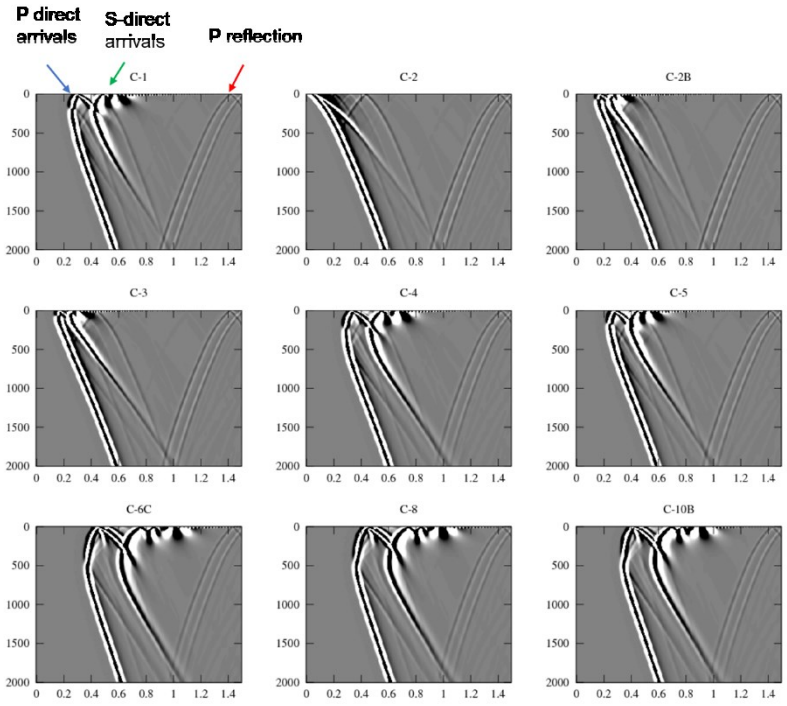

Figure 10: Synthetic DAS records for nine source locations using the model shown in Fig. 9. The P reflection arrivals are weak compared to the direct P arrivals, owing to the magnitude of velocity jump being not sufficiently large and width of reflection zone at 2.8–3.0 km depth.

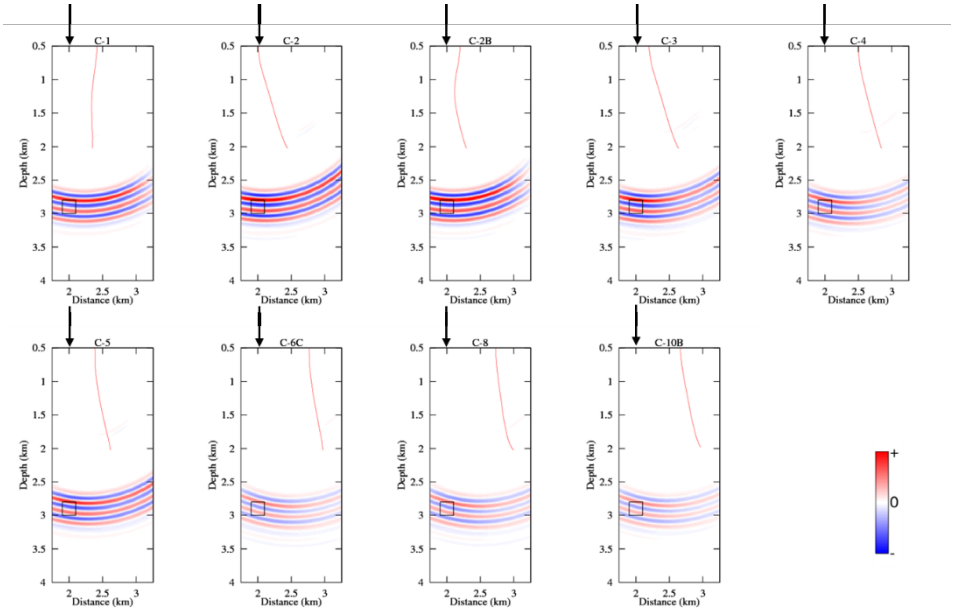

Figure 11: Migration test using the calculated theoretical up-going arrivals in Fig. 10. The rectangular light blue area shown in Fig. 8 is the true location of the reflection zone. The vertical force as the seismic source is shown by a black arrow. The migrated image is well concentrated in depth, but the horizontal accuracy is not well resolved due to the narrow aperture of the source and receivers.

6. DISCUSSION

By using active sources at nine locations, we recognize intense up-going arrivals for C3, C4, C5, C8, and C10B sources. Such up-going arrivals could be interpreted as PP reflections at 2.8–3.0 km depth. We migrated the up-going arrivals and obtained the top of the reflective zones at 0.5, 0.8, and 2.8 km depth. The horizontal width of the reflective zone was not well resolved. The overall width of the reflected zone could be as large as 500 m. The model assuming a box-shaped zone with a decrease in Vp and Vs is migrated at an almost accurate depth. The horizontal size and location showed migration smiles due to narrow apertures between the source and receiver pairs. The assumed velocity decrease was 1.0 km/s for both Vp and Vs. The intensity of theoretical reflections compared to the direct P arrivals was not so large and might imply that the velocity jump was much larger. If the velocity decrease was larger than 1.0 km/s, the zone at 2.8–3.0 km depth might be a fracture zone filled with fluid, possibly a geothermal reservoir. A granite-like dike intrusion was another candidate for a deep reflective zone. However, the possibility of making a velocity jump higher than 1.0 km/s by such a dike intrusion is scarce. Further studies, using FWI for velocity jumps and the width of reflective zones, are required.

Through two field studies in the Medipolis and Ohnuma geothermal fields in Japan, our DAS seismic method in the borehole could efficiently image areas of seismically reflected zones suggesting a high possibility of geothermal reservoirs. The suggested locations by migration were accurate in depth, but the horizontal location was less accurate, probably because of the narrow source-receiver aperture.

7. CONCLUSIONS

We carried out a third geothermal seismic study using the DAS system and active sources at the Ohnuma geothermal power plant in September 2020. We installed an optical fiber system for the DTS and DAS measurements and 26 surface seismometers on the surface of the site. We placed the optical fiber down to a depth of 1,973 m in the O-13R borehole. The temperature was measured as 240 ℃ at around 1,130 m depth using the DTS mode. We operated an IVI EnviroVibe seismic source at nine locations. We repeated the frequency sweep of 10–75 Hz 480 times a day for nine days. To improve the S/N, we stacked the DAS data and correlated the seismic records with the source signatures. By stacking for a long duration, we obtained excellent DAS records down to the bottom of the boreholes. Using reverse-time migration of observed and synthetic DAS seismic sections, we recognized intense seismic reflections from 2.8–3.0 km depth, suggesting the possibility of geothermal reservoirs. The velocity decrease in this zone was probably more than 1 km/s, suggesting the possible presence of a fluid-filled fracture zone.

In conclusion, through two successful field studies in the Medipolis and Ohnuma geothermal fields in Japan, the DAS seismic method in the borehole could efficiently image areas of seismically reflected zones suggesting a high possibility of the presence of geothermal reservoirs at intense seismic reflectors. The suggested locations by migration exhibit small (*i. e.*, +/-100 m) depth determination errors; however, the horizontal location is less accurate, probably owing to the observation geometry (narrow source-receiver aperture).

ACKNOWLEDGMENTS

This study was supported by the New Energy and Industrial Technology Development Organization (NEDO). We greatly appreciate Mitsubishi Materials Corporation for their kind permission for fieldwork in their power plant. Mr. Kimura provided us with Schlumberger hDVS measurements. YK Engineering Co. and Fujitsu Research Institute Co. provided DAS data. WELMA Co. provided us with a borehole fiber-optic system and measured the temperatures in the borehole. The staff of the Kawasaki Geological Engineering Co. and Daiwa Exploration and Consulting Co. assisted our surface seismological measurements during the field study. The IVI EnviroVibe operation was performed by JGI Inc.

REFERENCES

Hartog, A. H. [2017] An introduction to distributed optical fiber sensors, RC Press.440. pp.

Kasahara, J., Hasada, Y., and Yamaguchi, T. [2019a] Seismic imaging of supercritical geothermal reservoir using full-waveform inversion method, Proceedings, 44th Workshop on Geothermal Reservoir Engineering, Stanford University, Stanford, CA.

Kasahara, J., Hasada, Y, Kuzume, H., Fujise, Y. and Yamaguchi, T. [2019b] Seismic feasibility study to identify supercritical geothermal reservoirs in a geothermal borehole using DTS and DAS, EAGE extended abstract, EAGE 2019 Annual meeting, London.

Kasahara, J., Hasada, Y., Kuzume, H., Mikada, H., and Fujise, Y. [2020a] The second seismic study at the geothermal field in southern Kyushu, Japan using an optical fiber system and surface geophones, 44th Workshop on Geothermal Reservoir Engineering, Stanford University, Stanford, CA.

Kasahara, J., Hasada, Y., and Kuzume, H. [2020b] Possibility of high Vp/Vs zone in the geothermal filed suggested by the P-to-S conversion, 44th Workshop on Geothermal Reservoir Engineering, Stanford University, Stanford, CA.

Kubota, Y. [1985] Conceptional model of the north Hachmantai-Yakeyama geothermal area, Journal of Geothermal Society of Japan, **7**(3), 231-245.

Kubota, Y. [1988] Natural convention system at the Ohnuma-Sumikawa geothermal field, Northeastern Japan, 10th NZ Geothermal Workshop, 73-78.

Kubota, Y., Hatakeyama, K., Banba, M., Kato, H. [1989] Chemical changes of Ohnuma geothermal fluid since operation and related reservoir management, Journal of JGEA (Japan Geothermal Energy Association), **26**(1), 1-20.

Lindsey, N., Martin, E. R., Dreger, D.S., Freifeld, B., Cole, S., James, S., R., Biondi, B.L., and Ajo-Franklin J. B. [2017] Fiber-Optic network observation of earthquake wavefields, Geophysical Res. Letter, 10.10002/2017GL075722.

Mellors, R., Sherman, C. T., Ryerson, R., Morris, J., Messerly, J., Yu, C., Allen, G. and Ichinose, G. [2018] Modeling Potential EGS Signals from a Distributed Fiber Optic Sensor Deployed in a Borehole, Stanford Geothermal Workshop 2018.

NEDO [2008, 2009, 2010] Report of Geothermal Development Promotion, East of Ikeda Lake No. C-2-10, First, Second and Third phases.

Trainor-Guitton, W., Guitton, A., Jreij, S.F., Powers, H., Sullivan, C.B., Simmons, J., & PoroTomo Team [2018] 3D Imaging from vertical DAS fiber at Brady's Natural Laboratory, 43rd Workshop on Geothermal Reservoir Engineering

Yora, M., Wakita, K., and Honda, S. [1973] Exploration of Onuma geothermal field, northern Japan, Journal of JGEA (Japan Geothermal Energy Association), **10**(4), 27-44.

Yora, M, [1976] Drilling of Onuma geothermal wells, specially O-3Rb, Journal of JAPT (Japanese Association of Petroleum Technology), **41**(5), 13-19.

Yora, M., Watanabe, K., Ito, J., Wakita, K., Kubota, Y. [1977] On the geothermal system of the northern Hachimantai, Mining Geology, **27**, 233-244.

Wang., H., Z., Feigl, K. L., Thurber, C. H., and Mellory, R. J. [2018] Ground motion response to an ML 4.3 earthquake using co-located distributed acoustic sensing and seismometer arrays, Geophysical J. Int., **213**, 2020-2036.